

# Different glacier status with atmospheric circulations in Tibetan Plateau and surroundings

Tandong Yao<sup>1,2\*</sup>, Lonnie Thompson<sup>1,3</sup>, Wei Yang<sup>1</sup>, Wusheng Yu<sup>1</sup>, Yang Gao<sup>1</sup>, Xuejun Guo<sup>1</sup>, Xiaoxin Yang<sup>1</sup>, Keqin Duan<sup>1,2</sup>, Huabiao Zhao<sup>1</sup>, Baiqing Xu<sup>1</sup>, Jiancheng Pu<sup>2</sup>, Anxin Lu<sup>1,2</sup>, Yang Xiang<sup>1</sup>, Dambaru B. Kattel<sup>1</sup> and Daniel Joswiak<sup>1</sup>

The Tibetan Plateau and surroundings contain the largest number of glaciers outside the polar regions<sup>1</sup>. These glaciers are at the headwaters of many prominent Asian rivers and are largely experiencing shrinkage<sup>2</sup>, which affects the water discharge of large rivers such as the Indus<sup>3,4</sup>. The resulting potential geohazards<sup>5,6</sup> merit a comprehensive study of glacier status in the Tibetan Plateau and surroundings. Here we report on the glacier status over the past 30 years by investigating the glacial retreat of 82 glaciers, area reduction of 7,090 glaciers and mass-balance change of 15 glaciers. Systematic differences in glacier status are apparent from region to region, with the most intensive shrinkage in the Himalayas (excluding the Karakorum) characterized by the greatest reduction in glacial length and area and the most negative mass balance. The shrinkage generally decreases from the Himalayas to the continental interior and is the least in the eastern Pamir, characterized by the least glacial retreat, area reduction and positive mass balance. In addition to rising temperature, decreased precipitation in the Himalayas and increasing precipitation in the eastern Pamir accompanied by different atmospheric circulation patterns is probably driving these systematic differences.

Although some glaciological studies have been done in the Tibetan Plateau (TBP) and surroundings<sup>7–15</sup>, a region with a total glacial area of ~100,000 km<sup>2</sup> (Supplementary Table S1), the recent controversies<sup>7,16,17</sup> concerning glacial shrinkage in the Himalayas emphasize the necessity for a more comprehensive study. In addition, more concrete *in situ* observation data will help to recheck the results of a positive glacial mass balance of ~7 Gt yr<sup>-1</sup> in Tibet and Qilian Shan, which might be from uncertainty or misinterpretation of Gravity Recovery and Climate Experiment data<sup>7</sup>.

Under the progresses of the Third Pole Environment programme<sup>18</sup>, an integrated assessment of glacier status in and around the TBP over the past 30 years can now be provided. Data for this assessment come from studying the glacial area reduction of 7,090 glaciers, with an area of approximately 13,363.5 km<sup>2</sup> in the 1970s and approximately 12,130.7 km<sup>2</sup> in the 2000s (with a <5% uncertainty; see Supplementary Information) using topographic maps and satellite images from Landsat-MSS/TM/ETM+, ASTER and LISS (Supplementary Tables S2 and S3 and Figs S1 and S2). Eighty-two glaciers were also studied for glacial retreat using *in situ* observations and previous studies (Supplementary Table S4) and 15 glaciers have undergone intensive study of glacial mass balance by *in situ* measurement (Supplementary Tables S5 and S6 and Figs S3–S15).

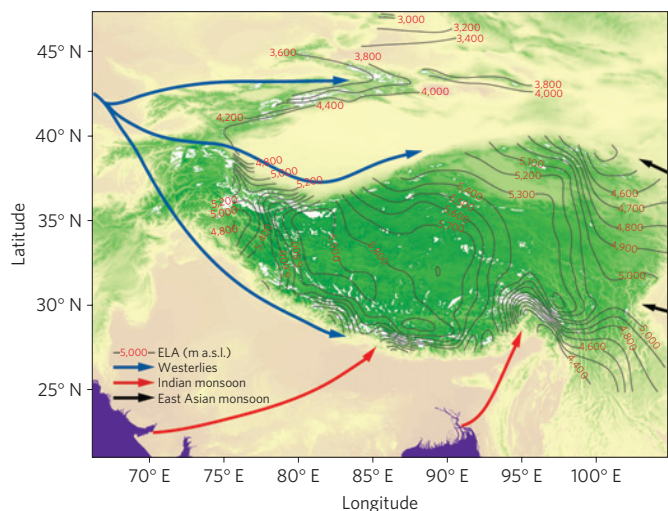


**Figure 1** | Distribution of glaciers and ELAs in and around the TBP<sup>11</sup>, which are mainly under the dominance of the Indian monsoon and westerlies, with limited influence from the East Asian monsoon. Note the increased glacier concentration and lower ELAs in the monsoon-dominated southeastern TBP and the westerlies-dominated Pamir regions, compared with the sparse glacial distribution and high ELAs in the continental-climate-dominated interior.

Present atmospheric circulation patterns over the TBP and surroundings are characterized by the Indian monsoon in the summer and the westerlies in the winter (Fig. 1). These two circulation systems, combined with the huge topographic landform, exert climatic controls on the distribution of existing glaciers. The East Asian monsoon also influences glaciers on the eastern margin, such as the Mingya Gongga and those in the eastern Qilian Mountains. The interior of the TBP is less influenced by the Indian monsoon and westerlies and dominated more by continental climatic conditions. As shown in Fig. 1, the high concentration and low equilibrium line altitudes (ELAs) of glaciers in the southeastern TBP and the eastern Pamir regions result from high precipitation from the Indian monsoon and westerlies, respectively, whereas more sparse glacier distribution and higher ELAs in the continental-climate-dominated interior are the consequences of limited water-vapour source from both these air masses.

To systematically and comprehensively assess glacier status in and around the TBP, we divided glaciers into seven regions,

<sup>1</sup>Key Laboratory of Tibetan Environmental Changes and Land Surface Processes, Institute of Tibetan Plateau Research, Chinese Academy of Sciences, Beijing 100101, China, <sup>2</sup>State Key Laboratory of Cryosphere Sciences, Chinese Academy of Sciences, Lanzhou 730000, China, <sup>3</sup>Byrd Polar Research Center and School of Earth Sciences, Ohio State University, Columbus, Ohio 43210, USA. \*e-mail: tdyao@itpcas.ac.cn.

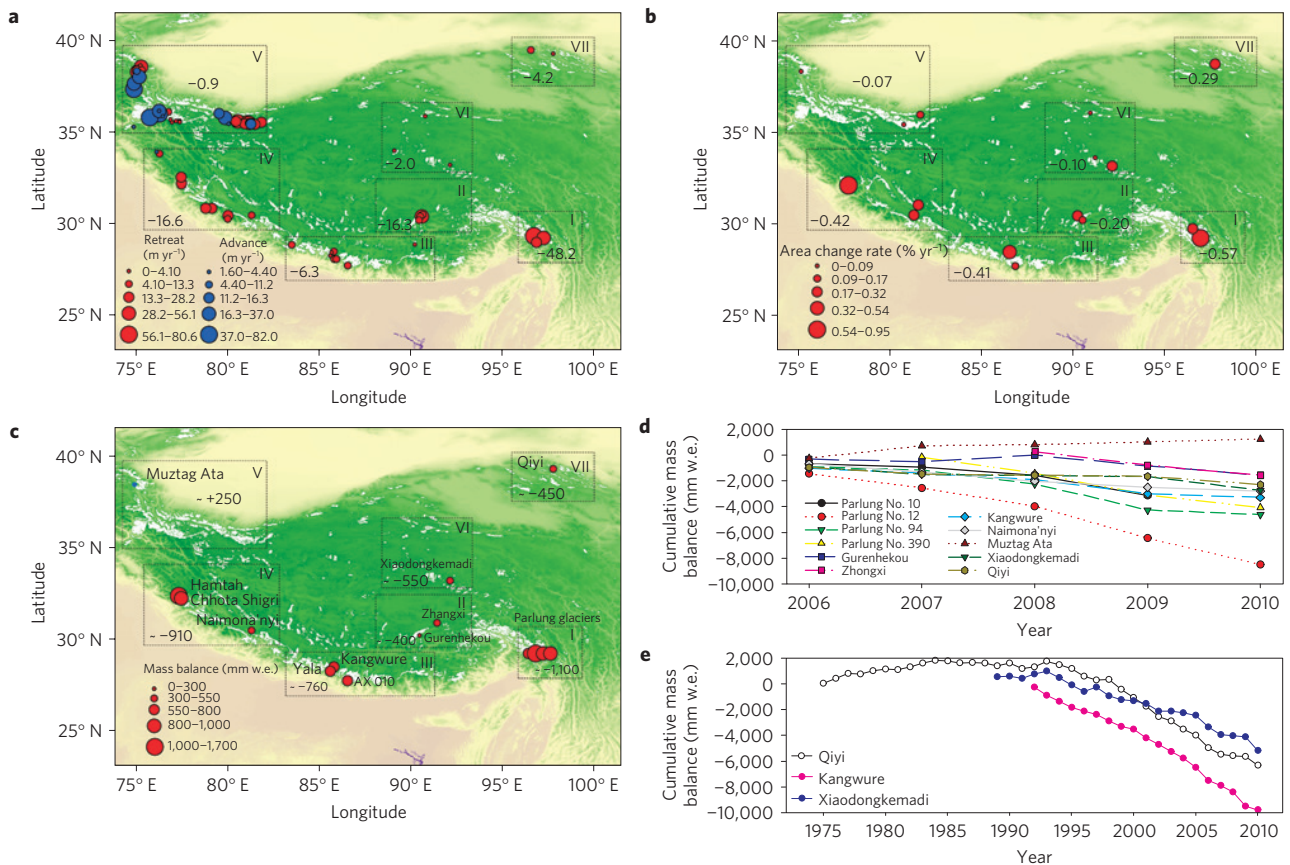


**Figure 2 | Spatial and temporal patterns of glacier status in the TBP and surroundings.** **a**, Glacier retreat for 82 glaciers (Supplementary Table S4). **b**, Area reduction for 7,090 glaciers (Supplementary Tables S2 and S3 and Fig. S1). **c**, Mass balance for 15 glaciers (Supplementary Table S5). Glaciers are categorized into seven regions and marked clockwise with Roman numerals in **a–c**. **d**, Cumulative mass balance for 11 glaciers in 2006–2010 (Supplementary Table S6 and Figs S3–S13). **e**, Cumulative mass balance for the three longest time series of glacier mass-balance measurements along transect 1 (Supplementary Table S7 and Figs S14 and S15).

indicated clockwise as I–VII in Fig. 2. This classification allows for an ideal geographic representation of glaciers in the TBP and surroundings, with one region each in the northeast and northwest, two in the centre and three in the Himalayas (southeastern TBP, central Himalayas and western Himalayas), which is the focus of many of the recent debates on glacier melt rates<sup>7,16,17</sup>. The seven regions can also be categorized climatically into three transects: transect 1, southwest–northeast oriented (including regions III, II, VI and VII), with the weakening Indian monsoon influence northward; transect 2, southeast–northwest oriented (including regions I, II and V), with the weakening Indian monsoon towards the interior and the strengthening westerlies towards the northwest; and transect 3, along the Himalayas (including regions I, III and IV), with stronger monsoon influence in the east and weaker monsoon influence in the west.

Transect 3 (the Himalayas) shows the most extreme glacial shrinkage based on the reduction both of glacier length and area (Fig. 2a,b and Supplementary Tables S2–S4). The shrinkage is most pronounced in the southeastern TBP (region I), where the length decreased at a rate of  $48.2 \text{ m yr}^{-1}$  and the area was reduced at a rate of  $0.57\% \text{ yr}^{-1}$  during the 1970s–2000s. The rate of glacial shrinkage decreases from the southeastern TBP (region I) to the interior (regions II and VI). A decreasing trend is discernible on both sides (regions III and VII) to the interior (regions II and VI) along transect 1. The smallest rate of glacier contraction is observed in the eastern Pamir regions (region V), with a retreat rate of  $0.9 \text{ m yr}^{-1}$  and area-reduction rate of  $0.07\% \text{ yr}^{-1}$ .

Mass balance is a direct and reliable indicator of glacier status. More than 20 glaciers have been measured for mass balance in the TBP and surroundings, but only 15 have been measured over three consecutive years (Supplementary Tables S5 and S6 and Figs S3–S13). Figure 2c shows the spatial pattern of the average annual mass balance of these 15 glaciers in the seven regions along the three transects. Similar to the variations in glacial length and area, the most negative mass balances occur along the Himalayas (transect 3), ranging from  $-1,100$  to  $-760 \text{ mm yr}^{-1}$  with an average of  $-930 \text{ mm yr}^{-1}$ . Along transect 2, the mass balance is not so negative, ranging from  $-1,100 \text{ mm yr}^{-1}$  in region I to  $-400 \text{ mm yr}^{-1}$  in region II, then becoming positive in region VII ( $+250 \text{ mm yr}^{-1}$ ). Along transect 1, the least negative mass balance is in the interior of region II.

Eleven of the fifteen glaciers have been continuously measured (from 2006 to 2010), thus enabling systematic studies by region (Fig. 2d; Supplementary Tables S5 and S6 and Figs S3–S13). Ten of the glaciers generally exhibit negative mass balance. The glacier with the most negative mass balance is the Parlung No. 12 Glacier ( $29^\circ 18' \text{ N}$ ,  $96^\circ 54' \text{ E}$ ) in the Parlung River Basin in the southeastern TBP (region I), with an average of  $-1,698 \text{ mm yr}^{-1}$ . In contrast to the other ten glaciers, the Muztag Ata Glacier in the eastern Pamir regions (region V) had a positive mass balance in four of the past five observation years.

Based on mass-balance measurements of the Qiyi, Xiaodongkemadi and Kangwure glaciers, starting from 1975, 1989 and 1992 respectively, and reconstructions along transect 1 (Fig. 2e; Supplementary Table S7 and Figs S14 and S15), we present an extended

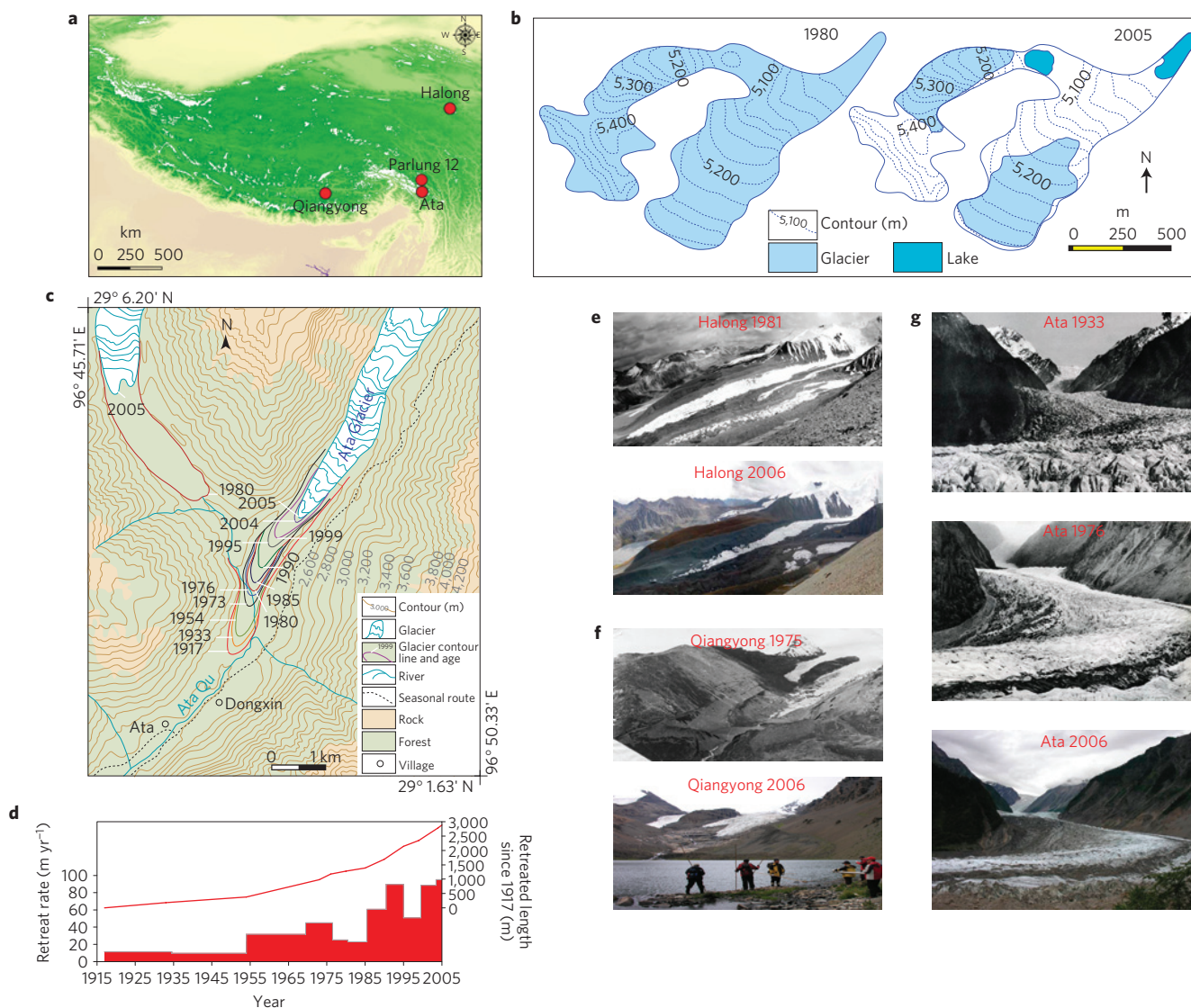


**Figure 3 | Case studies of glacial retreat.** **a**, The locations of studied glaciers. **b**, Area reduction of the Parlung No. 12 Glacier. **c,d**, Variations of the Ata Glacier since 1917. **e-g**, Glacial variation from comparison of photos of the Halong, Qiangyong and Ata glaciers, respectively. Panel **e**: top image © 1981 courtesy of Matthias Kuhle; bottom image © 2005 Greenpeace/Dan Novis; Panel **g**: top image reproduced with permission from ref. 21, © 1933 Wiley.

history. Mass balances of the Qiye and Xiaodongkemadi glaciers were positive until the early 1990s, then turned increasingly negative over time. The values associated with the Kangwure Glacier have been increasingly negative since 1992. In general, all these glaciers show an accelerating trend of more negative mass balance since the early 1990s.

Several glaciers in the TBP and surroundings were targeted for case studies (Fig. 3). The photos in Fig. 3b,d clearly demonstrate intensive glacial shrinkage. Photographs taken in 1981 and 2006 of the Halong Glacier (34° 46' N, 99° 30' E, Fig. 3b; ref. 19) reveal a significant reduction in length. *In situ* observations indicate that the retreat averaged 10 m yr<sup>-1</sup> during those 25 years. Photos of the Qiangyong Glacier (29° 57' N, 90° 09' E), which were published in 1976 (ref. 20), are compared with our 2006 photos (Fig. 3c). From these we can ascertain that the length has retreated at an average rate of 4 m yr<sup>-1</sup> during this period.

The Ata Glacier (29° 10' N, 96° 48' E), with a length of 16.7 km and an area of 13.8 km<sup>2</sup>, is on the southern slope of Mount Kangri Karpo in the southeastern TBP (Fig. 3d). The glacier was photographed in 1933 (ref. 21), 1976 (ref. 20) and 2006 (this study). We studied this glacier in detail using the historical photos, *in situ*

observations and the 1917 1:125,000 topographic map compiled by the US Army ([www.lib.utexas.edu/maps/ams/china](http://www.lib.utexas.edu/maps/ams/china); Fig. 3f,g). The glacial reduction averaged less than 20 m yr<sup>-1</sup> between 1917 and 1954, increased to more than 30 m yr<sup>-1</sup> from 1955 to 1984, increased again to more than 60 m yr<sup>-1</sup> after 1985 and exceeded 80 m yr<sup>-1</sup> in 2005/2006. The history of the Ata Glacier thus illustrates the largest amplitude of glacial retreat and reveals an accelerating trend in retreat since the 1990s.

A comparative study was done on the Parlung No. 12 Glacier, which has a length of 0.6 km and an area of 0.21 km<sup>2</sup> (2005 data) and is located on the northern slope of Mount Kangri Karpo (Fig. 3a). From 1980 to 2005, it retreated by ~700 m and its area reduced by ~55.3% (Fig. 3e). During field observations from 2006 to 2010, the glacier thinned by 9.5 m (21.1%) based on measuring stakes and its ice volume reduced by  $2.0 \times 10^6$  m<sup>3</sup> (38.7%) based on ground-penetrating radar measurements. If this rate continues, the Parlung No. 12 Glacier will disappear within either 25 years (based on ice-volume-reduction rates) or 35 years (based on ice-thickness-thinning rates). In contrast, the Ata Glacier will not disappear in the near future given its larger size and overall length. This implies a large-scale glacial behaviour with global

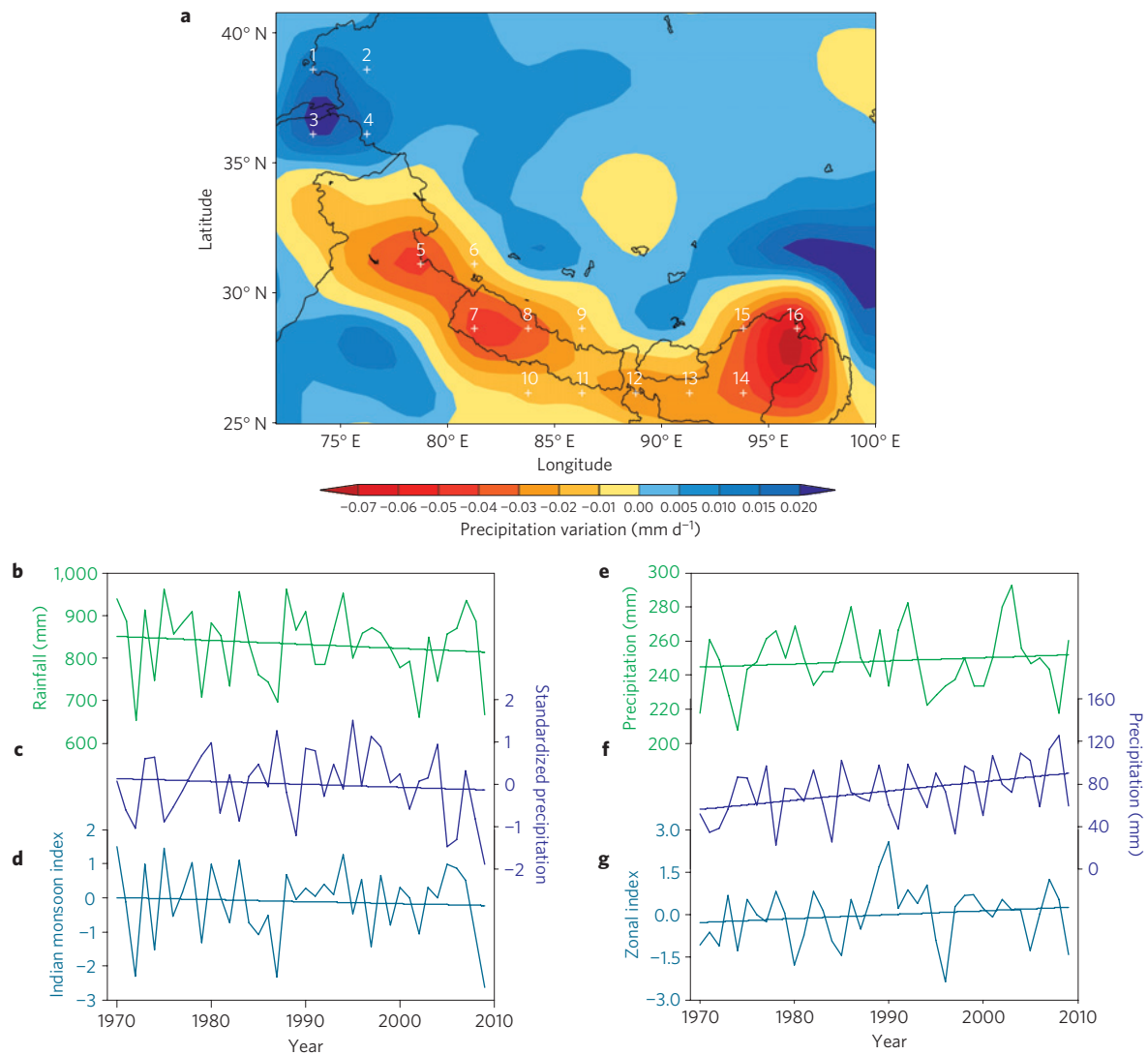


**Figure 4 | Precipitation patterns in the Himalayas and eastern Pamir regions.** **a**, Precipitation trends for 1979–2010 from the GPCP. Plus symbols indicate grid centres (Supplementary Figs S17 and S18). **b**, All-India rainfall (June–September). **c**, Standardized June–September precipitation from Linzhi, Zayu and Bomi in the southeastern TBP. **d**, Indian monsoon index for June–September<sup>30</sup>. **e**, Annual precipitation in Pamir regions and central Asia. **f**, Annual precipitation at Taxkorgan in the eastern Pamir regions. **g**, Zonal index for the Northern Hemisphere<sup>29</sup>. Time series in **b–g** cover the period 1970–2009. Straight lines indicate the linear trends.

warming such that smaller glaciers retreat faster than larger ones (Supplementary Fig. S2).

Temperature rise<sup>22,23</sup> contributes to glacial shrinkage over the TBP. Other factors are also important for glacier status, including size, type (temperate, polythermal or cold), condensation levels, sublimation, topography and debris cover, or a combination of many factors<sup>14,24</sup>. Climatic differences between low and high altitudes involve important issues relating to warming. An increasing warming trend at higher elevations has been observed over the TBP (ref. 22) and the warming rate increases with elevation before becoming quite stable with a slight decline near the highest elevations<sup>23</sup>. The rate of warming is highest between 4,800 and 6,200 m above sea level (a.s.l.) (ref. 23), which includes the ablation altitudes of almost all glaciers on the TBP. However, this is still not conclusive and more observations are necessary. Glaciers are mostly temperate in the southeastern TBP and on the southern slope of the Himalayas, whereas in other regions mentioned earlier the glaciers are primarily cold. This may also contribute to the observed differences in glacier status. However, the systematic differences suggest a precipitation pattern driven by atmospheric

circulation. Figure 4a shows the large-scale pattern of precipitation from the Global Precipitation Climatology Project (GPCP, [www.esrl.noaa.gov/psd/data/gridded/data.gpcp.html](http://www.esrl.noaa.gov/psd/data/gridded/data.gpcp.html)) over the TBP and surroundings. There is strong evidence that precipitation from 1979 to 2010 decreased in the Himalayas and increased in the eastern Pamir regions. The all-India rainfall (June–September; [www.tropmet.res.in](http://www.tropmet.res.in); Fig. 4b) and standardized June–September precipitation at three stations Linzhi (2,992 m a.s.l.), Zayu (2,328 m a.s.l.) and Bomi (2,736 m a.s.l.) in the southeastern TBP (Fig. 4c) confirm the decreasing precipitation in the Himalayas from the GPCP. The annual precipitation in the eastern Pamir regions and central Asia ([www.cru.uea.ac.uk](http://www.cru.uea.ac.uk); Fig. 4e) and at the Taxkorgan station (Fig. 4f) also confirms the increasing precipitation trend in the eastern Pamir based on the GPCP data. Recent studies found that the Indian monsoon is weakening<sup>25,26</sup> and the westerlies are strengthening<sup>27</sup>, which can influence changes in precipitation patterns<sup>28</sup>. The decreasing trend of the Indian monsoon index (Fig. 4d) suggests that the precipitation decrease in the Himalayas may be linked to the weakening Indian monsoon, whereas the increasing zonal index<sup>29</sup> (Fig. 4) reveals that the precipitation

increase in the eastern Pamir is linked to the strengthening westerlies. The general patterns of mass balance over the TBP follow atmospheric circulation patterns (Supplementary Fig. S16).

The glacier status in the TBP and surroundings varies systematically from region to region: the Himalayas shows the greatest decrease in length and area, and the most negative mass balance, whereas the eastern Pamir shows the least reduction in length and area, and positive mass balance. The main cause for this regional trend is probably decreasing/increasing precipitation in the Himalayas/eastern Pamir regions, which results from changes in the two different atmospheric circulation patterns, that is, the weakening Indian monsoon and strengthened westerlies. Under the present warming conditions, glacier shrinkage might further accelerate in the Himalayas whereas glaciers might advance in the eastern Pamir regions. Potential consequences of glacier changes would be unsustainable water supplies from major rivers<sup>3,4</sup> and geohazards (glacier-lake expansion, glacier-lake outbursts and flooding)<sup>5,6</sup>, which might threaten the livelihoods and wellbeing of those in the downstream regions.

## Methods

**Mass-balance measurement and calculation.** Mass balance, specific net ablation and net accumulation were calculated from measurements in the field. Net-ablation measurements were carried out using the measuring-stake method in the ablation zone. Net-accumulation measurements were carried out using snow-pit measurements in the accumulation zone. In the measuring-stake method, snow- and ice-surface changes caused by negative net balance were manually determined on measuring stakes. Snow-pit measurements involved mapping of visible stratigraphic features. For both methods, the measurements were made at the end of each ablation season (generally at the end of September or beginning of October) and snow densities were also measured for water-equivalent (w.e.) calculation.

For a given glacier, the overall glacier mass balance  $B$  is calculated as

$$B = \frac{\sum_{i=1}^n b_i s_i}{S} \quad (\text{in mm})$$

where  $b_i$  is the specific mass balance (net ablation or net accumulation) of the given altitudinal range  $i$  over map area  $s_i$  and  $S$  is the total glacial area. For a given altitudinal range,  $b_i$  is obtained from the corresponding net-ablation or net-accumulation measurements.

**Glacial length observation.** Annual variations of glacial length were observed and calculated by repeated observations between the benchmark locations and glacier termini. The uncertainty of present field observation by differential global positioning systems is negligible. The uncertainty of the previous field observations is determined by the number of *in situ* measurements. Our measurements in the field comprise five points for each small glacier (<2 km<sup>2</sup>) and nine points for larger glaciers. The uncertainty of this method is estimated at 5–10%.

**Glacial area analysis.** Among the glacial area analysis of 16 river basins in seven regions, nine are gleaned from the literature and seven are based on our own studies (four have not been published). Topographic maps, aerial photography and data from Hexagon KH-9, LISS-III/LISS-IV, Landsat MSS, Landsat TM/ETM+, ALOS AVNIR-2, Terra ASTER and SRTM DEM were considered in this study. As topographic maps, aerial photography and remote sensing data were taken at different times and different resolutions, they were first orthorectified, co-registered and correlated. The TM3/TM5, TM4/TM5 band-ratio methods were used to automatically delineate the glacial area in our study. After automated delineation, we visually checked and manually adjusted the regions for shadow, seasonal snow, turbid/frozen/multihued proglacial lakes and debris cover. The mapping uncertainty of our studies is less than 3% for clean-ice glaciers and 4% for debris-covered glaciers. The methods and results from previous studies include manual delineation based on visual interpretation from digitized topographic maps and/or false-colour composite satellite images, supervised classification, band-ratio method, normalized different snow index and normalized different water index. The uncertainty of those studies is  $\pm 2$ –3% for clean-ice glaciers and  $\pm 3$ –4% for debris-covered glaciers for ASTER and Landsat TM (see the third paragraph in the Supplementary Information).

Received 21 November 2011; accepted 14 May 2012;  
published online 15 July 2012

## References

1. Yao, T. *et al.* *Map of Glaciers and Lakes on the Tibetan Plateau and the Surroundings* (Xi'an Cartographic Publishing House, 2008).
2. Yao, T., Pu, J., Lu, A., Wang, Y. & Yu, W. Recent glacial retreat and its impact on hydrological processes on the Tibetan Plateau, China, and surrounding regions. *Arct. Antarct. Alp. Res.* **39**, 642–650 (2007).
3. Immerzeel, W.W., Beek, L. P. H. & Bierkens, M. F. P. Climate change will affect the Asian water towers. *Science* **328**, 1382–1385 (2010).
4. Kaser, G., Großhauser, M. & Marzeion, B. Contribution potential of glaciers to water availability in different climate regimes. *Proc. Natl Acad. Sci. USA* **107**, 20223–20227 (2010).
5. Richardson, H. D. & Reynolds, J. M. An overview of glacial hazards in the Himalayas. *Quat. Int.* **65/66**, 31–47 (2000).
6. Kääb, A. *et al.* Remote sensing of glacier- and permafrost-related hazards in high mountains: An overview. *Nat. Hazards Earth Syst. Sci.* **5**, 527–554 (2005).
7. Jacob, T., Wahr, J., Pfeffer, W. T. & Swenson, S. Recent contributions of glaciers and ice caps to sea level rise. *Nature* **482**, 514–518 (2012).
8. Ding, Y., Liu, S., Li, J. & Shangguan, D. The retreat of glaciers in response to recent climate warming in western China. *Ann. Glaciol.* **43**, 97–105 (2006).
9. Li, X. *et al.* Cryospheric change in China. *Glob. Planet. Change* **62**, 210–218 (2008).
10. Bolch, T. *et al.* The state and fate of Himalayan glaciers. *Science* **336**, 310–314 (2012).
11. Shi, Y., Liu, C. & Kang, E. The glacier inventory of China. *Ann. Glaciol.* **50**, 1–4 (2009).
12. Li, Z., Sun, W. & Zeng, Q. Measurements of glacier variation in the Tibetan Plateau using Landsat data. *Remote Sens. Environ.* **63**, 258–64 (1998).
13. Fujita, K., Ageta, Y., Pu, J. & Yao, T. Mass balance of Xiao Dongkemadi glacier on the central Tibetan Plateau from 1989 to 1995. *Ann. Glaciol.* **31**, 159–163 (2000).
14. Scherler, D., Bookhagen, B. & Strecker, M. R. Spatially variable response of Himalayan glaciers to climate change affected by debris cover. *Nature Geosci.* **4**, 156–159 (2011).
15. Fujita, K. & Nuimura, T. Spatially heterogeneous wastage of Himalayan glaciers. *Proc. Natl Acad. Sci. USA* **108**, 14011–14014 (2011).
16. Cogley, J., Kargel, J. S., Kaser, G. & van der Veen, C. Tracking the source of glacier misinformation. *Science* **327**, 522–522 (2010).
17. Bagla, P. No sign yet of Himalayan meltdown, Indian report finds. *Science* **326**, 924–925 (2009).
18. Yao, T. & Greenwood, G. A new polar program. *EOS* **90**, 515–515 (2009).
19. Greenpeace & Kuhle, M. Yellow River source at risk under climate change. ([http://activism.greenpeace.org/yellowriver/yrs-english\\_web.pdf](http://activism.greenpeace.org/yellowriver/yrs-english_web.pdf), 2007).
20. Li, J. *et al.* *Glaciers in Tibet* (in Chinese) (Science Press, 1986).
21. Ward, F. K. The Himalaya East of the Tsangpo: A paper read at the evening meeting of the society on 30 April 1934. *Geograph. J.* **84**, 369–397 (1933).
22. Liu, X. & Chen, B. Climatic warming in the Tibetan Plateau during recent decades. *Int. J. Climatol.* **20**, 1729–1742 (2000).
23. Qin, J., Yang, K., Liang, S. & Guo, X. The altitudinal dependence of recent rapid warming over the Tibetan Plateau. *Climatic Change* **97**, 321–327 (2009).
24. Xu, B. *et al.* Deposition of anthropogenic aerosols in a southeastern Tibetan glacier. *J. Geophys. Res.* **114**, D17209 (2009).
25. Wu, B. Weakening of Indian summer monsoon in recent decades. *Adv. Atmos. Sci.* **22**, 21–29 (2005).
26. Thompson, L.G. *et al.* Abrupt tropical climate change: Past and present. *Proc. Natl Acad. Sci. USA* **103**, 10536–10543 (2006).
27. Zhao, H. *et al.* Deuterium excess record in a southern Tibetan ice core and its potential climatic implications. *Clim. Dynam.* **38**, 1791–1803 (2012).
28. Naidu, C.V. *et al.* Is summer monsoon rainfall decreasing over India in the global warming era? *J. Geophys. Res.* **114**, D24108 (2009).
29. Li, J. & Wang, J. X. L. A modified zonal index and its physical sense. *Geophys. Res. Lett.* **30**, 1632 (2003).
30. Wang, B., Wu, R. & Lau, K.-M. Interannual variability of the Asian summer monsoon: Contrasts between the Indian and the western North Pacific-East Asian monsoons. *J. Clim.* **14**, 4073–4090 (2001).

## Acknowledgements

This work is supported by the NSFC (41190081, 40810019001), the CAS (External Cooperation Program GJHZ0960 and SAFEA International Partnership Program for Creative Research Teams) and the MOST (2005CB422004). We thank Q. Ye for help preparing Fig. 3.

## Author contributions

All authors contributed extensively to this work.

## Additional information

The authors declare no competing financial interests. Supplementary information accompanies this paper on [www.nature.com/natureclimatechange](http://www.nature.com/natureclimatechange). Reprints and permissions information is available online at [www.nature.com/reprints](http://www.nature.com/reprints). Correspondence and requests for materials should be addressed to T.Y.